ELSEVIER

Biochimica et Biophysica Acta 1466 (2000) 139–150

BIOCHIMICA ET BIOPHYSICA ACTA
BBA

www.elsevier.com/locate/bba

Functional studies of a chimeric protein containing portions of the Na^+/glucose and Na^+/*myo*-inositol cotransporters

Michael J. Coady [a,*], Fairouze Jalal [a], Pierre Bissonnette [a], Mathilde Cartier [a], Bernadette Wallendorff [a], Guy Lemay [a,b], Jean-Yves Lapointe [b,c]

[a] *Groupe de Recherche en Transport Membranaire, Université de Montréal, Montreal, Que. H3C 3J7, Canada*
[b] *Département de Microbiologie, Université de Montréal, Montreal, Que. H3C 3J7, Canada*
[c] *Département de Physique, Université de Montréal, Montreal, Que. H3C 3J7, Canada*

Received 2 November 1999; received in revised form 29 February 2000; accepted 29 February 2000

Abstract

We obtained cDNA chimeras between Na/glucose cotransporter (SGLT1) and the homologous Na^+/*myo*-inositol cotransporter (SMIT) by creating random chimeras in plasmids. Of 12 chimeras, two were functional when expressed in *Xenopus laevis* oocytes but, upon sequencing, only one of them (C1) produced an actual chimeric protein. In C1, the first 69 amino acids of SGLT1 were replaced by the corresponding 50 amino acids of SMIT. C1 transports the same sugars as does SGLT1. C1's affinity for all sugar substrates was systematically increased by a factor of 3.3 ± 0.4 but the V_{max} was diminished by a factor of 15–40. In contrast, the cotransport affinity for Na^+ was unchanged. The surface expression of C1 was one seventh that of SGLT1, which explains part of the reduced V_{max} and implies a significant reduction in turnover rate. N-terminal truncated constructs of SGLT1 cDNA showed that deleting amino acids 2–14 does not affect cotransporter activity, but that the pentapeptide $T_{14}RPVET_{19}$ is important for normal levels of SGLT1 current. The main result of a kinetic analysis of the systematic increase in apparent affinity for sugars, together with the intact Na apparent affinity, suggests enhanced access to the sugar binding site in C1.

Keywords: SGLT1; SMIT; Chimera; Transporter

1. Introduction

The first mammalian cotransporter cDNA to be cloned was the Na^+/glucose cotransporter [1]. Since SGLT1 cDNA can be expressed at high levels in *Xenopus laevis* oocytes, where both steady-state and transient currents can be measured, this system has been used extensively for analyzing the kinetics of this cotransporter [2–7]. This approach has, however, provided little information about the nature of the binding sites for Na^+ and sugars or the mechanism by which the transporter functions.

Some knowledge about the structure of this transporter has been obtained from sequence alignments of SGLT1 to homologous proteins. SGLT1 belongs to a group of proteins that transports a wide range of substrates (e.g. glucose, iodine, proline and pantothenic acid) and displays considerable diversity in the carboxyl halves of the sequences [8,9]. In contrast, the amino terminal halves display considerable similarity, though not within their extreme terminal regions.

* Corresponding author. Fax: +1-514-343-7146;
E-mail: coady@ere.umontreal.ca

0005-2736/00/$ – see front matter
PII: S0005-2736(00)00186-3

Within the family of transporters homologous to SGLT1, the Na^+/*myo*-inositol cotransporter (SMIT) displays a high degree of identity (46%) and similarity (80%) to SGLT1 [10]. The physiological function of this protein is well established and it has been shown to display substrate-dependent currents when expressed in *Xenopus* oocytes [11]. Both SGLT1 and SMIT are specifically inhibited by phlorizin, albeit with different K_i values, and the proteins display different substrate specificities although their substrates are chemically similar. The creation of chimeras between homologous proteins has been used to deduce structure–function relationships for different membrane proteins, such as G-protein-coupled receptors [12,13], ion channels [14] and transporters [15,16]. In the case of SGLT1, a single paper reports the production of a chimera composed of amino acids 1–380 of porcine SGLT2 (low-affinity Na^+/glucose cotransporter) and 381–662 of porcine SGLT1 [17]. This chimera maintained the affinity and the sugar specificity of SGLT1, but the affinity for Na^+ was intermediate between that of the two original proteins. The possibility that the sugar binding site was determined by the carboxyl terminal half of the protein was later confirmed by the observation of some sugar transport through a cDNA construct expressing only the last five transmembrane segments of the protein [18].

In this study, we employed a method previously described for rapidly creating multiple chimeras between related proteins [19], which requires cleavage of a circular, recombinant plasmid between two homologous cDNA inserts placed 'head-to-toe'. We focus here on a functional chimera where the initial 69 amino acids of SGLT1 were replaced by the corresponding 50 amino acids of SMIT. This chimera (C1) transports αMG but not *myo*-inositol and has been functionally characterized in detail.

2. Materials and methods

2.1. Chimera generation

Preparation of chimeric transporters was done as described by Moore and Blakely [19]. One initial construct was pSPORT–SMIT, generously provided by Dr. Moo Kwan (Johns Hopkins School of Medicine, Baltimore, MA). The other was pMT21–SGLT1 [6] which expresses human SGLT1 in eukaryotic cells. Site-directed mutagenesis was used to create a *Mlu*I site in the 5′-untranslated region of SGLT1. The mutated recombinant was then cleaved with *Mlu*I followed by a partial cleavage with *Pst*I (due to a *Pst*I polymorphism near the 3′ end of our human SGLT1) to yield a linear fragment containing a small gap between the *Pst*I and *Mlu*I sites immediately upstream of the full-length SGLT1 insert. The full-length SMIT insert was removed from pSPORT using *Mlu*I and *Sse*8387I, and ligated into the cleaved pMT21–SGLT1. The pMT21–SMIT–SGLT1 DNA was then linearized at two unique restriction sites between the two cDNAs (*Sna*BI and *Xba*I) and dephosphorylated, and the linear DNA was purified from an agarose gel. 50–100 ng of purified DNA were transformed by heat shock into 200 μl of competent DH5α bacteria. Bacterial colonies which imported and recircularized the linearized plasmid were selected using carbenicillin (50 μg/ml). Plasmids were purified from these colonies and those which displayed an insert size between 2400 and 3100 bp were used for intranuclear injection of *Xenopus* oocytes. The plasmids were subsequently analyzed by restriction enzyme mapping to locate the approximate position of the SMIT–SGLT1 junction. Dideoxy sequencing (Sequenase v2.0, Amersham Pharmacia Biotech, Baie d'Urfé Canada) was performed to determine the precise junction between the portions of SMIT and SGLT1 in selected plasmids.

2.2. SGLT1 deletion mutants

The creation of a series of deletion mutants at the amino terminus was performed using the polymerase chain reaction. The following oligonucleotides (Alpha DNA, Montreal, Canada) were used: 5′-Trunc, CATGGTGGCAGCGGAATTCAGGCTCG; 3′-Trunc#1, ACCTGGAGCCCCAAGACCACCGCG; 3′-Trunc#2, ACCACCGCGGTCACCCGGCCT; 3′-Trunc#3, CGGCCTGTTGAGACCCACGAGCTCATTC; 3′-Trunc#4, CACGAGCTCATTCGCAATGCAGCCGAT. The 5′-Trunc oligo was used in each reaction and coded for the reverse complement of the 5′-untranslated region and the starting methionine codon. Deletion mutants SGLT1Δ2–4 (i.e. amino acids 2–4 are deleted),

SGLT1Δ2–9, SGLT1Δ2–14 and SGLT1Δ2–19 were created by performing PCR [20] using the 5′-Trunc oligonucleotide with the 3′-Trunc#1, 3′-Trunc#2, 3′-Trunc#3 and 3′-Trunc#4 oligonucleotides, respectively. Sequencing results showed that the SGLT1Δ2–4 deletion mutant actually produced an SGLT1Δ2–6 deletion: it was used and is listed as such below. Sequencing of the other deletion mutants indicated that the products were as originally planned.

2.3. Oocyte injection and maintenance

Oocytes were removed from *Xenopus laevis* adults (Xenopus One, Ann Arbor, MI) under anesthesia with 0.13% 3-aminobenzoic acid ethyl ester; the cells were defolliculated, injected and maintained as previously described [21]. Each plasmid preparation was diluted to 65 ng/μl in water containing 65 ng/μl of a recombinant pMT21 vector which expressed secreted alkaline phosphatase (pMT21–SEAP), for injection of 4.6 nl aliquots into oocytes. The detection of SEAP activity in the external milieu of isolated oocytes was used to select oocytes which were expressing nuclear-injected DNA [22]. Later experiments replaced SEAP with a cDNA that expressed green fluorescent protein [23] for identification of oocytes which expressed the injected DNA [24]. No differences have been observed between glucose-induced currents in oocytes expressing either 300 pg of pMT21–SGLT1 plasmid or 10 ng of in vitro transcribed SGLT1 mRNA aside from greater variability in the level of expressed currents when DNA is expressed. No glucose-induced currents were seen in either uninjected oocytes or water-injected oocytes.

2.4. Two microelectrode voltage-clamp

Oocyte currents were measured with the two microelectrode voltage-clamp technique as described [21]. Only cells with resting membrane potentials more negative than −35 mV were used. The standard bath solutions contained (in mM): NaCl 90, KCl 3, $MgCl_2$ 0.82, $CaCl_2$ 0.74, HEPES 5, pH 7.6. Oocytes were held at −50 mV and transmembrane currents were measured in response to changes in bath sugar, Na^+, and phlorizin concentrations. A data acquisition system (R.C. Electronics, Santa Barbara, CA) was used to send voltage pulse protocols and simultaneously record current and voltage signals. Eleven alternating 150 ms duration pulses separated by 500 ms periods at the resting potential (−50 mV) were used; the voltage range covered was from −175 to +75 mV. Current and voltage traces were analyzed by averaging the signal in a window of 20 ms positioned at the end of the pulse, well after all capacitative transients have decayed.

2.5. Phlorizin binding measurements

Phlorizin (Pz) binding studies were performed using control (non-injected) and mRNA-injected oocytes at 5–7 days following injection. Oocytes were preincubated (8–12 per vial) at room temperature for 15 min in Barth's solution prior to assay. The preincubation medium was replaced with 0.5 ml of medium containing tracer amounts of ^{3}H-phlorizin (2 μCi/ml, specific activity 55 Ci/mmol, New England Nuclear, Boston, MA) and incubated for another 15 min period. Binding was stopped by rinsing four times with 2 ml of ice-cold Barth's solution. Oocytes were then transferred individually into scintillation vials and dissolved by agitation in 0.2 ml 10% SDS for 4 h after which 5 ml of Beta-Blend scintillation cocktail (ICN, Montreal Canada) was added. Tritium levels were measured using liquid scintillation counting. Specific binding on SGLT1-expressing oocytes is completely displaced by excess cold phlorizin (50 μM).

Statistical significance was assessed using Student's paired or unpaired t-test, as appropriate.

3. Results

3.1. Production of chimeric cDNAs

After transformation with the linearized pMT21–SMIT–SGLT1 plasmid, 23 carbenicillin-resistant bacterial colonies were isolated. Restriction digest analysis revealed that 11 of the recombinant plasmids contained inserts which were too long to code for a true chimeric cDNA and that all recombination in the other 12 plasmids occurred within or prior to the first 80 amino acids of SGLT1. The recombinant plasmids were injected into oocytes which were sub-

sequently exposed to α-methylglucose (αMG) or *myo*-inositol (substrates for SGLT1 and SMIT, respectively). None of the oocytes evinced significant currents (>5 nA) upon application of 5 mM *myo*-inositol, but two of the cDNA clones produced measurable currents upon exposure to 5 mM αMG; the other 10 clones were not further studied. Of the two positive clones (C1 and C5), one (C5) produced a protein identical to SGLT1 since the recombination occurred in the untranslated region of SGLT1, whereas the other (C1) expressed a true chimeric protein. Sequencing of the C1 cDNA revealed a protein largely identical to SGLT1, but where the N-terminal 69 amino acids of SGLT1 were replaced by the first 50 amino acids of SMIT (Fig. 1A); recombination occurred somewhere within the DNA coding for the subsequent six amino acids, which are identical in the two sequences. Analysis of the C1 and SGLT1 sequences produced similar hydropathy values [25] and suggested a similar membrane topology for both C1 and SGLT1 (Fig. 1B), indicating that the extracellular N-terminal region and the two initial transmembrane domains of C1 are derived from SMIT.

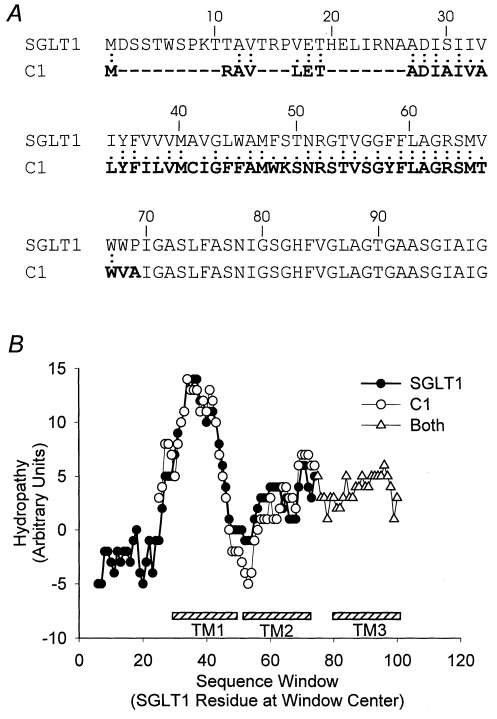

Fig. 1. Comparison of the SGLT1 and C1 protein sequences. The chimera C1 is identical to SGLT1 except that the first 69 amino acids of SGLT1 are replaced by the first 50 amino acids of SMIT. (A) Alignment of the initial amino acid sequences of SGLT1 and C1. The bold characters indicate the portion of the C1 sequence that is derived from SMIT. The numbers refer to position in the SGLT1 sequence. Similar and identical residues are indicated by one or two dots, respectively. (B) Hydropathic profile of the amino terminal region of the protein sequences of SGLT1 and C1. Proposed membrane-spanning domains are shown by striped bars. The analysis was performed using windows between 11 and 21 amino acids.

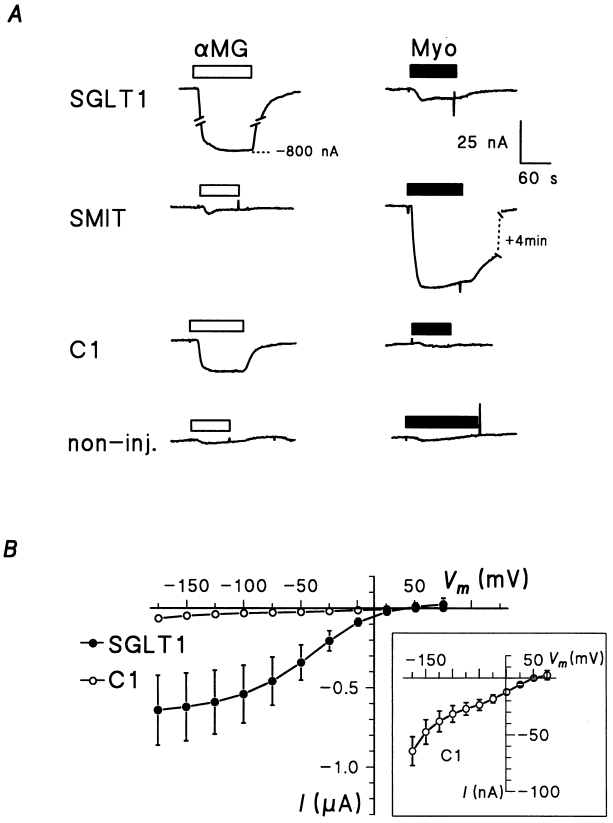

Fig. 2. Sugar-induced currents via SGLT1 and C1. (A) Recordings of αMG- and *myo*-inositol-induced currents in SGLT1-, SMIT- and C1-expressing oocytes as well as in control oocytes. DNA-injected oocytes were exposed to 5 mM αMG or *myo*-inositol in saline Barth's solution and the membrane potential was held at −50 mV. (B) Current–voltage relationships of the steady-state currents in C1- and SGLT1-expressing oocytes which are induced by addition of 1 mM glucose ($n=6$). The inset shows the C1 current–voltage relationship using a diminished ordinate scale.

3.2. Sugar-induced currents

Fig. 2A shows the currents recorded when non-injected oocytes and oocytes expressing SGLT1,

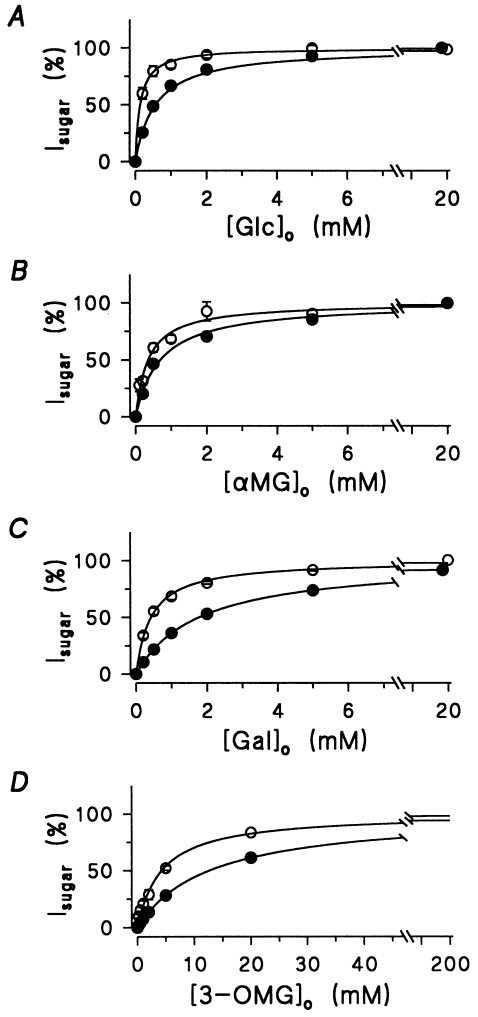

Fig. 3. Sugar activation of the cotransport current. Currents were measured in DNA-injected oocytes held at −50 mV with perfusion of varying external concentrations of different sugars. The [Na^+] was 88 mM and the [sugar] ranged from 200 μM to 20 mM. For each oocyte, currents were first normalized to 100% = current at 20 mM substrate. For each sugar concentration, these data were combined from four to six oocytes to produce mean values (shown with error bars representing S.E.M.). The combined data were fitted to a Michaelis–Menten equation to derive K_m and I_{max} values. For presentation, the currents have been normalized with the calculated I_{max} values set at 100%, in order to better compare the two curves. Closed circles represent oocytes expressing SGLT1; open circles represent oocytes expressing C1. Glc, glucose; Gal, galactose; 3-OMG, 3-*O*-methylglucose.

SMIT or C1 were perfused with solutions containing 5 mM αMG or 5 mM *myo*-inositol. Perfusion with 5 mM *myo*-inositol caused inward currents of 50 nA in SMIT-expressing oocytes and of 10 nA in SGLT1-expressing oocytes, but no current was seen with C1-expressing oocytes. Perfusion of SGLT1- and C1-expressing oocytes with 5 mM αMG produced inward currents that were absent in both control and SMIT-expressing oocytes. The αMG-induced current in C1-expressing oocytes was 15 to 40 times smaller than that in SGLT1-expressing oocytes, with observed variations in this ratio being primarily due to different batches of oocytes. The current/voltage (*I–V*) relationships of the D-glucose dependent currents (shown in Fig. 2B) were deduced by subtracting currents measured in the absence of 1 mM glucose from those measured in the presence of glucose. As others have previously shown [2,11], the glucose-induced inward current of SGLT1 increases with increasingly negative membrane potentials between +50 and −100 mV and seems to reach a maximal level at highly negative potentials. The glucose-induced current for C1 also increases from +50 to −100 mV, but increases even more between −100 and −175 mV. Interestingly, the published *I–V* relationship for SMIT behaves in a similar manner [11].

To examine the effects of altering the amino terminal region of the chimera on the glucose-binding site, C1- and SGLT1-expressing oocytes were incubated with varying concentrations of αMG. As shown in Fig. 3B, the activation of the C1 cotransport current by αMG can be described by a Michaelis–Menten curve characterized by an affinity significantly higher than that seen with SGLT1. From independent measurements, the K_m of C1 for αMG at −50 mV was 0.37 ± 0.05 mM while the equivalent

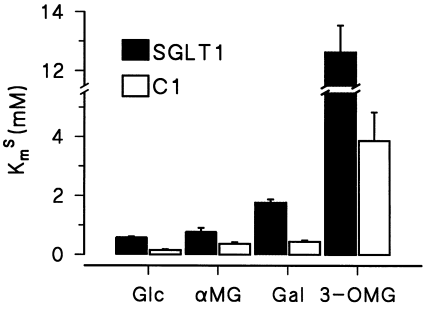

Fig. 4. Individual sugar affinities of SGLT1 and C1. The affinities of C1 and SGLT1 for the four sugars tested were determined with oocytes held at −50 mV. All values represent means ± S.E.M. of the affinity constants measured from four to six oocytes for both C1 and SGLT1.

value for SGLT1 was 0.77 ± 0.14 mM, ($P < 0.05$). Thus, despite the diminution of the αMG-induced currents observed by converting SGLT1 to C1, the chimeric protein is characterized by an increased affinity for the specific substrate of SGLT1.

3.3. Affinities for different sugars

We examined whether the selectivity amongst different substrates (see Fig. 3) known to be transported by SGLT1 was also altered, indicative of whether the selectivity of the sugar binding site was changed. In Fig. 4, the affinity constants of C1 and SGLT1 for various sugars are shown, measured at −50 mV. For both SGLT1 and C1, $K_m^{D\text{-glucose}} < K_m^{\alpha MG} < K_m^{D\text{-galactose}} < K_m^{3\text{-}O\text{-methylglucose}}$. In addition to having the same selectivity sequence of sugars as seen for SGLT1, the ratio between the SGLT1 and C1 K_m values for any sugar were always between 2 and 4.2 (average ± S.D. = 3.3 ± 0.4). The uniform change in affinities produced by altering the N-terminus of SGLT1 suggests that the modification did not alter the protein's structural moieties which differentiate between the sugars used here, despite the overall changes in K_m values.

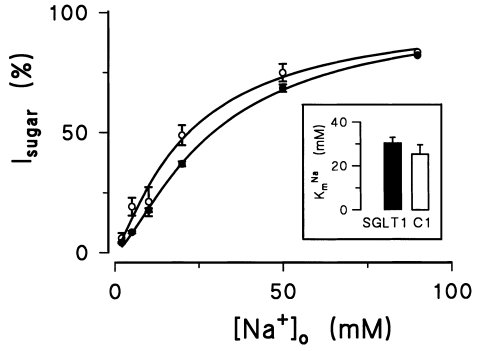

Fig. 5. Sodium affinities of SGLT1 and C1. αMG-dependent currents in C1- and SGLT1-expressing oocytes were measured with varying external concentrations of Na^+. The [αMG] was 5 mM and $[Na^+]$ ranged from 200 μM to 90 mM. Data shown are the mean ± S.E.M. of currents measured from seven oocytes for both C1 (open circles) and SGLT1 (closed circles). The currents have been normalized with respect to the calculated maximal current at 100% in order to better compare the two curves. The inset displays the affinity constants derived from a Hill analysis of the data.

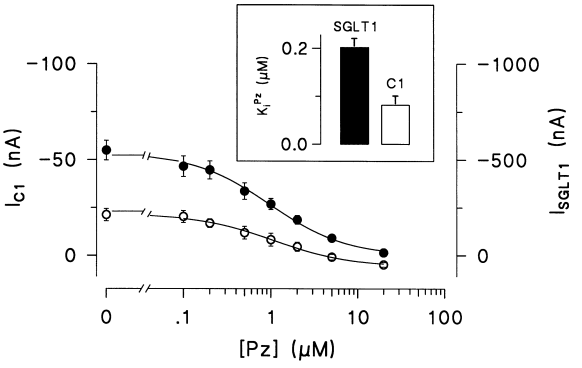

Fig. 6. Phlorizin sensitivity of cotransport currents. The αMG-induced steady-state current was inhibited by perfusion with external phlorizin in saline Barth's solution. The holding potential was −50 mV, the external αMG concentration was 5 mM and the [phlorizin] ranged from 100 nM to 20 μM. Data shown represent means ± S.E.M. for C1 (open circles, $n = 5$) and SGLT1 (closed circles, $n = 9$). The inset shows the inhibition constants derived from a competitive inhibition model.

3.4. Na affinities

Fig. 5 illustrates the activation of cotransport currents by the external Na^+ concentration ($[Na^+]_o$) in the presence of 5 mM αMG. This data was analyzed using the Hill equation. Despite markedly different levels of current for SGLT1 and C1 (26 ± 3 nA for C1 vs. 680 ± 70 nA for SGLT1 at 90 mM Na, $n = 7$ each), the activation by $[Na^+]_o$ was slightly sigmoidal ($n_H = 1.2$ for C1 and 1.4 for SGLT1 at −50 mV) for both cotransporters and the average K_m values for Na^+ were indistinguishable ($K_m = 25 \pm 4$ mM for C1 and 31 ± 2 mM for SGLT1). Furthermore, the Na^+ K_m values for SGLT1 and C1 both varied with membrane potential in identical fashion (data not shown). In comparison, the Na K_m value for SMIT, when perfused with *myo*-inositol, is slightly higher than that described for SGLT1 and is almost voltage-independent [11]. We conclude that Na interacts with C1 in a manner very similar to that seen with SGLT1.

3.5. Phlorizin sensitivities

To determine sensitivity to phlorizin, current was measured from voltage-clamped SGLT1- and C1-expressing oocytes in the presence of 5 mM αMG, 90 mM NaCl and various concentrations of phlorizin.

Fig. 6 shows that increasing the concentration of phlorizin decreased the αMG-induced steady-state current. Analysis of the data, using a competitive inhibition model employing the values for αMG affinities derived above (0.37 mM for C1 and 0.77 mM for SGLT1), provided estimates of the apparent K_i values for phlorizin. As can be seen in Fig. 6, the two curves are very parallel as can be expected when the inhibitor K_i has changed in proportion to the substrate K_m. The best K_i values fitting the data of Fig. 6 are 0.07 ± 0.01 μM for C1 and 0.13 ± 0.01 μM for SGLT1, i.e. in proportion to the respective K_m values. By comparison, the K_i for SMIT is 64 μM [11]. Thus, as was seen for sugar substrates, replacing the N-terminus of SGLT1 with that of SMIT increased the affinity for phlorizin.

3.6. Turnover rates

We sought to determine whether the low level of currents associated with C1 could be accounted for by a decrease in the number of transport proteins at the cell surface. Glucose-induced currents were measured from oocytes which expressed SGLT1 or C1, following which radiolabelled phlorizin was used to detect the surface density of transport molecules

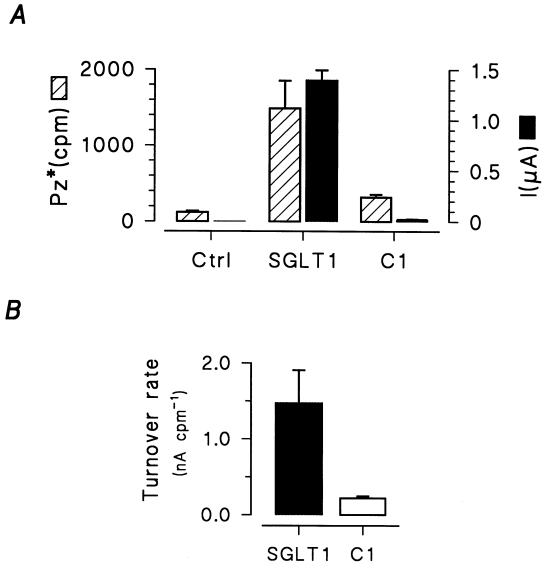

Fig. 7. Phlorizin binding to C1 and SGLT1. (A) The level of phlorizin binding is shown for groups of oocytes alongside the currents measured from the same oocytes. (B) Turnover rates for SGLT1 and C1 were derived from the data shown in A.

(Fig. 7A). To calculate the number of surface transporters, the cpm count must be corrected for the different phlorizin affinities of SGLT1 and C1. This would generally be done by measuring binding of labelled phlorizin in the presence of different concentrations of non-labelled phlorizin, but this approach was unfeasible here due to the low levels of radioactivity bound to C1-expressing oocytes. In the case of SGLT1, however, Pz binding could be determined at different total concentrations of Pz and the affinity measured was 0.13 ± 0.08, which was not different from the K_i measured in Fig. 6. Therefore, we measured phlorizin binding to C1-expressing oocytes at a single tracer concentration of phlorizin and derived the number of binding sites (B_{max}) using the K_i value obtained from the results shown in Fig. 6, employing the formulae given below. The current-derived K_i values for both C1- and SGLT1-expressing oocytes and the measurements from radiolabelled phlorizin binding to the oocytes (cpm) were used for calculating the number of binding sites as follows:

$$\text{cpm} = \frac{B_{max}[\text{Pz}]}{K_i + [\text{Pz}]} \quad (1)$$

Thus, B_{max} can be defined as

$$B_{max} = \text{cpm}\frac{(K_i + [\text{Pz}])}{[\text{Pz}]} \quad (2)$$

Although the C1-expressing oocytes shown in Fig. 7A displayed seven times less phlorizin binding than did SGLT1, the glucose-induced currents in C1-expressing oocytes were 48 times less than those in SGLT1-expressing cells. To account for the remaining difference in transport activity the turnover number, obtained by dividing the recorded currents by the phlorizin binding, must be seven times lower in C1 than in SGLT1 (Fig. 7B).

We investigated whether the differences in transport activity between SGLT1 and C1 were due to the altered amino acid sequence and not simply due to the diminished length of the amino terminus by creating four truncated SGLT1 mutant proteins. αMG-dependent currents were measured in oocytes that were expressing each of the deletion mutants and compared to those measured with full-length SGLT1. Deletion mutants SGLT1Δ2–6, SGLT1Δ2–9 and SGLT1Δ2–14 yielded currents that were indistinguishable from those of full-length SGLT1 (data

not shown). The affinities for Na^+ of these mutant proteins (SGLT1Δ2–6, $K_m = 27 \pm 2$ mM, $n = 4$; SGLT1Δ2–9, $K_m = 23 \pm 0.3$ mM, $n = 3$; SGLT1Δ2–14, $K_m = 27 \pm 2$ mM, $n = 4$) were similar to those measured for SGLT1 ($K_m = 31 \pm 2$ mM). The affinities for glucose were also unchanged by the deletions (SGLT1Δ2–6, $K_m = 0.63 \pm 0.03$ mM, $n = 9$; SGLT1Δ2–9, $K_m = 0.58 \pm 0.02$ mM, $n = 6$; SGLT1Δ2–14, $K_m = 0.52 \pm 0.03$ mM, $n = 6$ vs. a K_m of 0.58 ± 0.03 mM for SGLT1). In contrast, further deletion of amino acids 14–19 (SGLT1Δ2–19) produced substrate-dependent currents that were rarely measurable in oocytes and, when present, were on the order of 5 nA.

4. Discussion

As compared to other membrane proteins (e.g. potassium channels), very little is known about the structure–function relationship of 12–14 transmembrane domain cotransporters. Not only is crystal structure unavailable, but even the general function of specific portions of the primary sequence remains largely unknown. One way to gain access to this type of information is to create chimeric proteins between homologous cotransporters and to follow specific perturbations in several characteristic properties. In the case of the Na-glucose cotransporter family, one such chimera has been reported (between SGLT1 and SGLT2) which led to the suggestion that the sugar-binding site was located in the C-terminal half of the protein [17]. This was further supported by a study on a truncated SGLT1 where the last five C-terminal transmembrane segments were shown to form a Na-independent glucose transporter [18].

We found that successful chimera production is severely limited by the apparent fragility of the protein. Out of 12 chimeras produced, only one translated an actual chimeric protein which retained some functionality. In a recent study from our laboratory, we added three different epitope tags corresponding to about 10 amino acids at two different locations in the protein sequence and a single combination produced an active protein [26]. Single amino acid mutations were also found to inactivate the protein and cause glucose–galactose malabsorption syndrome [27]. The same type of low success rate in producing functional mutated transporters was found when a glycosylation site was introduced at various locations in the primary sequence in order to establish the actual membrane topology of the cotransporter [9]. We suspect that the susceptibility of this protein's activity to small changes in sequence may be due to a large change in conformation required of a protein whose function involves interaction with and translocation of three substrates; recently the first direct observation of this conformational change was reported [28]. For these reasons, we employed an in vivo recombination method to create chimeras between SMIT and SGLT1. This technique has several advantages in that it yields a large number of chimeras in a short time and the site of joining between the two proteins should be randomly located within homologous regions. The low rate of success at obtaining active chimeras prompted us to focus on comparing many functional characteristics of chimera C1 to those of SGLT1 rather than create additional chimeras; the low success rate also provides convincing evidence that a method of creating a relatively large number of random chimeras, as used here, is preferable to using site-directed mutagenesis and recombination to directly create chimeras.

4.1. Properties of C1

In the present study, we have compared several transport properties of C1 to the corresponding properties of SGLT1. The most intriguing finding is that the apparent affinity constants, for several types of sugars as well as for the inhibitor phlorizin, are increased by a factor of 2–4. On the other hand, the apparent affinity constants of SGLT1 and C1 for Na, at a saturating glucose concentration, are identical. Interpreting apparent affinity constants is not straightforward in the case of a cotransporter, like SGLT1, which must go through three binding reactions on each side of the membrane (generating a minimum of eight different states). In addition, although there is agreement that Na binds first at the extracellular surface [29], the binding order of the second Na ion and the glucose molecule is still debated [4,7,30]. Fig. 8 presents one possible model as proposed by Bennett and Kimmich [30] and for which we have recently provided some experimental evidence [7]. For reasons of clarity, we have com-

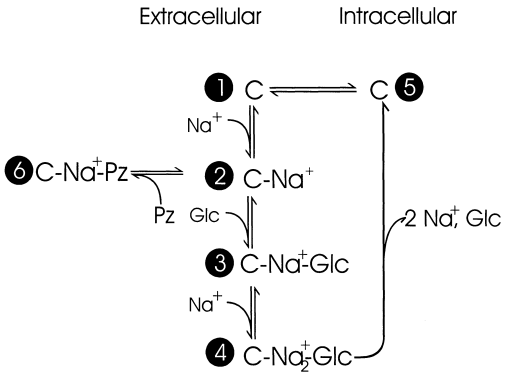

Fig. 8. Kinetic model of SGLT1 activity. A kinetic model of SGLT1 is shown where, for reasons of clarity, the Na leak currents have been omitted and the intracellular steps have been combined. Black circles indicate the individual conformational states.

bined the reactions where the Na ions and the glucose molecule are released on the intracellular side. We have also omitted the pathway corresponding to the small Na-leak current that corresponds to about 1% of the maximal Na-glucose current. As explained in the Appendix, the simplest means by which to explain a higher glucose affinity with a constant Na affinity (at saturating glucose) is to augment the rate constant for glucose binding (k_{23} in Fig. 8), which would be increased by a factor of 2–4 in the case of C1 with respect to the corresponding rate constant of SGLT1. This is fully consistent with the observed decrease in the phlorizin K_i as the binding of a competitive inhibitor is likely to follow the pathway for the binding of glucose. Altering the speed at which glucose may bind to the cotransporter without changing the binding site itself or its associated dissociation rate constant (k_{32}) explains why four different substrates with widely varying affinities all display affinity constants which are increased by a similar factor. The explanation for the decrease in turnover rate calculated for C1 is not straightforward at this point. A decrease in the maximal activity of the cotransporter must be related to one of the steps that were lumped together in the transitions from state 4 to 5 and from state 5 to 1 (see Fig. 8). Similarly, the *I–V* curve obtained at high Na and αMG concentrations reflects the voltage dependence of the same lumped steps. The resemblance noted between the *I–V* curve of C1 and SMIT suggests that, in these two cases, the resulting rate constants can be accelerated by hyperpolarization throughout the voltage range while, in the case of SGLT1, a voltage-insensitive step becomes rate-limiting at potentials more negative than −75 mV. This also indicates that the N-terminal region of SGLT1 contains a moiety which is involved in the saturation of activity as the membrane potential becomes quite negative.

4.2. Sequence comparison

Within the first 50 amino acids of SMIT (the SMIT-derived sequence that is found in C1), the level of identity between the amino acid sequence of C1 and the corresponding region of SGLT1 is 48%. The most striking difference between the primary structures of SGLT1 and C1 is in the extreme N-terminal, extracellular [9,26,31] region where the initial 26 amino acids of SGLT1 have very little similarity to their heptapeptide counterpart in SMIT. To examine whether the differences in functional activity between C1 and SGLT1 are due to this region of SGLT1 that is essentially absent from SMIT (and thus C1), we created a series of mutant forms of SGLT1 which bore deletions (of 5–18 amino acids) immediately following the initial methionine. Although amino acids 2–14 were removed without causing any apparent change to SGLT1 activity, there was very little αMG-induced current when SGLT1Δ2–19 was expressed in *Xenopus* oocytes (not shown), suggesting that the pentapeptide $_{15}$RPVET$_{19}$ plays an important role in the biosynthesis, folding or trafficking of SGLT1. This indicates that the shorter amino terminus of C1 may explain a portion of the low activity recorded for the chimera, but it should be noted that the N-terminal heptapeptide of C1 does contain the sequence $_5$LET$_7$, which is similar to part of the pentapeptide described above. This may explain why C1 displays considerably more current than that seen with SGLT1Δ2–19.

Binding of radiolabelled phlorizin to the oocytes showed that the surface density of SGLT1 was approximately seven times that of C1. The diminished number of C1 transporters at the plasma membrane may be due to decreased stability of the RNA or protein, or to incorrect processing or/and targeting of C1 to the plasma membrane. Simply switching the 5′ untranslated region of SGLT1 for that of SMIT may affect the level of protein translation since the

initial codon in SMIT is surrounded by a Kozak consensus sequence inferior to that of SGLT1 [32].

4.3. Comparison with other structure/function properties of SGLT1

The developing concept around the structure/function of SGLT1 is that the glucose-binding domain is mostly comprised of the last 5 transmembrane segments, while the Na binding sites are possibly located in the first half of the protein [17,18]. Although the N-terminal halves of SGLT1 and related Na^+ cotransport proteins might be expected to be involved in the transport of Na^+, based on their sequence similarities, the Na^+ affinity of C1 displays the same magnitude and voltage-dependence (data not shown) as does that of SGLT1. By comparison, SMIT has a higher Na^+ affinity and the K_m value is less voltage-dependent. These data suggest that the initial seventy amino acids of the N-terminal region of SGLT1, which are replaced in C1 by the equivalent region of SMIT, are not immediately involved in the binding of Na^+, in agreement with the results of Lo and Silverman [31] which suggested that the region between transmembrane helices IV and V plays a role in Na^+ binding and voltage-sensing. On the other hand, our observation that the replacement of the N-terminus has increased the glucose apparent affinity of SGLT1 might appear contradictory to the previous suggestion that the last 5 transmembrane spanning segments constitute the glucose transporter. However, our kinetic analysis (see Appendix) and the observation that phlorizin and four different substrates have experienced the same modification in their respective affinity indicates that it is the access to the binding site and not the binding site itself that is modified in C1 vs. SGLT1.

This study has shown that replacement of the first 69 amino acids of SGLT1 with the corresponding 50 amino acids of SMIT diminished the K_m for αMG and reduced the turnover rate by a factor of 7, but left the Na^+ affinity intact, indicating that the Na^+ binding site is unlikely to be located in the N-terminal region of SGLT1 that is different in C1. However, the specificity of binding amongst sugars was unchanged, suggesting that the sugar binding site itself was unaltered and that the extracellular N-terminal plays a role in favoring accessibility to the binding site.

Acknowledgements

This research was supported by a Medical Research Council of Canada grant (MT-10580) awarded to J.Y.L.

Appendix

To consider the effects of replacing the amino terminal region of SGLT1 with that of SMIT, we employ a simplified kinetic model (Fig. 8). Using the program of Falk et al. [33] to solve a set of steady-state reactions like those shown in Fig. 8, the Na influx is given by

$$J_{Na} = \frac{C_1 \cdot Glc \cdot Na^2}{C_6 + C_5 Na + C_3 GlcNa + C_4 Na^2 + C_2 \cdot Glc \cdot Na^2}. \quad (A1)$$

The definition of each constant term 'C_n' is given in Table 1. The apparent affinity constant for the substrate (Glc) can be defined as

$$K_m^{Glc} = \frac{C_6 + C_5 Na + C_4 Na^2}{C_3 Na + C_2 Na^2}. \quad (A2)$$

Under our experimental conditions, where K_m^{Glc} is measured in the presence of 90 mM Na (three times its apparent affinity at high [Glc]), it is useful to take

Table 1
Constants used in modeling SGLT1 kinetics

Model constant	Definition
C_1	$= k_{12}\ k_{23}\ k_{34}\ k_{45}\ k_{51}$
C_2	$= k_{12}\ k_{23}\ k_{34}\ (k_{45}+k_{51})$
C_3	$= k_{23}\ (k_{15}\ k_{34}\ k_{45}+k_{12}\ k_{43}\ k_{51}+k_{12}\ k_{45}\ k_{51}+ k_{34}\ k_{45}\ k_{51})$
C_4	$= k_{12}\ k_{34}\ k_{45}\ k_{51}$
C_5	$= k_{15}\ k_{21}\ k_{34}\ k_{45}+k_{12}\ k_{32}\ k_{43}\ k_{51}+ k_{12}\ k_{32}\ k_{45}\ k_{51}+k_{21}\ k_{34}\ k_{45}\ k_{51}$
C_6	$= k_{21}\ k_{32}\ (k_{43}+k_{45})(k_{12}+k_{51})$

the limit of Eq. A2 for very high extracellular [Na],

$$\lim_{Na\to\infty} K_m^{Glc} = \frac{C_4}{C_2} = \frac{k_{45}k_{51}}{k_{23}(k_{45}+k_{51})}. \quad (A3)$$

The apparent affinity constant for Na can be easily derived when Glc is assumed to be high in Eq. A1. This apparent Na affinity (at high Glc) is

$$\lim_{Glc\to\infty} K_m^{Na} = \frac{C_3}{C_2}$$

$$= \frac{k_{15}k_{34}k_{45} + k_{12}k_{43}k_{51} + k_{12}k_{45}k_{51} + k_{34}k_{45}k_{51}}{k_{12}k_{34}(k_{45}+k_{51})}. \quad (A4)$$

Given Eqs. A3 and A4, it can be seen that K_m^{Glc} is inversely proportional to k_{23}, the forward rate constant for substrate binding, while K_m^{Na} is completely independent of k_{23}. Then, the simplest way to change the K_m^{Glc} by a factor of 3 without changing K_m^{Na} is to act on k_{23}. Other possibilities certainly exist, but they would generally require a certain combination of rate constants that makes K_m^{Na} insensitive to this modification.

Another strong support for our contention that k_{23} explains the observed changes in substrate affinity is the observation of a parallel change in the phlorizin inactivation constant (K_i). Phlorizin is recognized as a competitive inhibitor against glucose for Na-glucose cotransport. Based on the equations describing competitive inhibition, Pz affects the substrate apparent affinity constant as follows:

$$K_m^{Glc} = K_{m\ (Pz=0)}^{Glc} * \left(1 + \frac{Pz}{K_i}\right) \quad (A5)$$

Given the model shown in Fig. 8, the inhibition constant for Pz in the presence of a high Na concentration is simply given by

$$K_i = \frac{k_{62}}{k_{26}} \quad (A6)$$

Fig. 6 shows that the phlorizin K_i must change in proportion with the substrate K_m in order to generate identical inhibition curves for C1 and SGLT1. The simplest explanation is that k_{26} for Pz, which corresponds to k_{23} for substrate binding, is increased by a factor of 2–4. Interestingly, the measurement of K_i for Pz does not depend on the other rate constants of the cycle.

References

[1] M.A. Hediger, M.J. Coady, T.S. Ikeda, E.M. Wright, Nature 330 (1987) 379–381.
[2] J.A. Umbach, M.J. Coady, E.M. Wright, Biophys. J. 57 (1990) 1217–1224.
[3] L. Parent, S. Supplisson, D.D. Loo, E.M. Wright, J. Membr. Biol. 125 (1992) 49–62.
[4] L. Parent, S. Supplisson, D.D. Loo, E.M. Wright, J. Membr. Biol. 125 (1992) 63–79.
[5] D.D. Loo, A. Hazama, S. Supplisson, E. Turk, E.M. Wright, Proc. Natl. Acad. Sci. USA 90 (1993) 5767–5771.
[6] X. Chen, M.J. Coady, F. Jackson, A. Berteloot, J.-Y. Lapointe, Biophys. J. 69 (1995) 2405–2414.
[7] X.Z. Chen, M.J. Coady, F. Jalal, B. Wallendorff, J.-Y. Lapointe, Biophys. J. 73 (1997) 2503–2510.
[8] J. Reizer, A. Reizer, M.H. Saier Jr., Biochim. Biophys. Acta 1197 (1994) 133–166.
[9] E. Turk, E.M. Wright, J. Membr. Biol. 159 (1997) 1–20.
[10] H.M. Kwon, A. Yamauchi, S. Uchida, A.S. Preston, A. Garcia-Perez, M.B. Burg, J.S. Handler, J. Biol. Chem. 267 (1992) 6297–6301.
[11] K. Hager, A. Hazama, H.M. Kwon, D.D. Loo, J.S. Handler, E.M. Wright, J. Membr. Biol. 143 (1995) 103–113.
[12] B.K. Kobilka, T.S. Kobilka, K. Daniel, J.W. Regan, M.G. Caron, R.J. Lefkowitz, Science 240 (1988) 1310–1316.
[13] R. Maggio, Z. Vogel, J. Wess, Proc. Natl. Acad. Sci. USA 90 (1993) 3103–3107.
[14] G.E. Kirsch, C.C. Shieh, J.A. Drewe, D.F. Vener, A.M. Brown, Neuron 11 (1993) 503–512.
[15] A. Pessino, D.N. Hebert, C.W. Woon, S.A. Harrison, B.M. Clancy, J.M. Buxton, A. Carruthers, M.P. Czech, J. Biol. Chem. 266 (1991) 20213–20217.
[16] S.K. Loewen, A.M. Ng, S.Y. Yao, C.E. Cass, S.A. Baldwin, J.D. Young, J. Biol. Chem. 274 (1999) 24475–24484.
[17] M. Panayotova-Heiermann, D.D. Loo, C.T. Kong, J.E. Lever, E.M. Wright, J. Biol. Chem. 271 (1996) 10029–10034.
[18] M. Panayotova-Heiermann, S. Eskandari, E. Turk, G.A. Zampighi, E.M. Wright, J. Biol. Chem. 272 (1997) 20324–20327.
[19] K.R. Moore, R.D. Blakely, Biotechniques 17 (1994) 130–135.
[20] M.P. Weiner, G.L. Costa, W. Schoettlin, J. Cline, E. Mathur, J.C. Bauer, Gene 151 (1994) 119–123.
[21] M.J. Coady, F. Jalal, X.Z. Chen, G. Lemay, A. Berteloot, J.-Y. Lapointe, FEBS Lett. 356 (1994) 174–178.
[22] A.G. Swick, M. Janicot, T. Cheneval-Kastelic, J.C. McLenithan, M.D. Lane, Proc. Natl. Acad. Sci. USA 89 (1992) 1812–1816.
[23] M. Chalfie, Y. Tu, G. Euskirchen, W.W. Ward, D.C. Prasher, Science 263 (1994) 802–805.
[24] M.J. Coady, G. Lemay, J.-Y. Lapointe, FASEB J. 10 (1996) A89.
[25] G. von Heijne, J. Mol. Biol. 225 (1992) 487–494.
[26] P. Bissonnette, J. Noel, M.J. Coady, J.-Y. Lapointe, J. Physiol. 520 (1999) 359–371.

[27] M.G. Martin, M.P. Lostao, E. Turk, J. Lam, M. Kreman, E.M. Wright, Gastroenterology 112 (1997) 1206–1212.
[28] D.D. Loo, B.A. Hirayama, E.M. Gallardo, J.T. Lam, E. Turk, E.M. Wright, Proc. Natl. Acad. Sci. USA 95 (1998) 7789–7794.
[29] G. Semenza, M. Kessler, M. Hosang, J. Weber, U. Schmidt, Biochim. Biophys. Acta 779 (1984) 343–379.
[30] E. Bennett, G.A. Kimmich, Biophys. J. 70 (1996) 1676–1688.
[31] B. Lo, M. Silverman, J. Biol. Chem. 273 (1998) 29341–29351.
[32] M. Kozak, Nucleic Acids Res. 15 (1987) 8125–8148.
[33] S. Falk, N. Oulianova, A. Berteloot, Biophys. J. 77 (1999) 173–188.